

Phase separation and suppression of critical dynamics at quantum transitions of itinerant magnets: MnSi and $(\text{Sr}_{1-x}\text{Ca}_x)\text{RuO}_3$

Y. J. Uemura,¹ T. Goko,^{2,1} I. M. Gat-Malureanu,^{1,3} J. P. Carlo,¹ P. L. Russo,¹ A. T. Savici,¹ A. Aczel,⁴ G. J. MacDougall,⁴ J. A. Rodriguez,⁴ G. M. Luke,⁴ S. R. Dunsiger,⁴ A. McCollam,⁵ J. Arai,² Ch. Pfleiderer,⁶ P. Böni,⁶ K. Yoshimura,⁷ E. Baggio-Saitovitch,⁸ M. B. Fontes,⁸ J. Larrea J.,⁸ Y. V. Sushko,⁹ and J. Sereni¹⁰

¹*Department of Physics, Columbia University, New York, New York 10027, USA*

²*Department of Physics, Tokyo University of Science, Noda, Chiba 278-8510, Japan*

³*Department of Science, SUNY Maritime College, Throggs Neck, New York, NY 10465, USA*

⁴*Department of Physics and Astronomy, McMaster Univ., Hamilton, ON, Canada*

⁵*Department of Physics, University of Toronto, Toronto M5S 1A7, Ontario, Canada*

⁶*Physik Department, Technische Universität München, D-85748 Garching, Germany*

⁷*Department of Chemistry, Kyoto University, Kyoto 606-8502, Japan*

⁸*Centro Brasileiro de Pesquisas Fisicas, Rua Xavier Sigaud 150 Urca, CEP 22290-180 Rio de Janeiro, Brazil*

⁹*Department of Physics and Astronomy, University of Kentucky, Lexington, KY 40506-0055, USA*

¹⁰*Lab. Bajas Temperaturas, Centro Atomico Bariloche, Bariloche, Argentina*

(Dated: September 1, 2018)

PACS numbers: 75.35.Kz 73.43.Nq 76.75.+i

Quantum phase transitions (QPTs) have been studied extensively in correlated electron systems. Characterization of magnetism at QPTs has, however, been limited by the volume-integrated feature of neutron and magnetization measurements and by pressure uncertainties in NMR studies using powdered specimens. Overcoming these limitations, we performed muon spin relaxation (μSR) measurements which have a unique sensitivity to volume fractions of magnetically ordered and paramagnetic regions, and studied QPTs from itinerant heli/ferro magnet to paramagnet in MnSi (single-crystal; varying pressure) and $(\text{Sr}_{1-x}\text{Ca}_x)\text{RuO}_3$ (ceramic specimens; varying x). Our results provide the first clear evidence that both cases are associated with spontaneous phase separation and suppression of dynamic critical behavior, revealed a slow but dynamic character of the “partial order” diffuse spin correlations in MnSi above the critical pressure, and, combined with other known results in heavy-fermion and cuprate systems, suggest a possibility that a majority of QPTs involve first-order transitions and/or phase separation.

Advances of materials preparation and characterization techniques have revealed complicated and sometimes unexpected phenomena near phase transitions and phase boundaries in correlated electron systems. Fascinating examples can be found in pressure-tuned crossover from ferro (or heli) magnetic to paramagnetic states in itinerant electron systems, such as MnSi [1, 2] and ZrZn₂ [3], as well as UGe₂ [4] which is associated with appearance of a superconducting state near the disappearance of ferromagnetism. MnSi exhibits magnetic order with

a spontaneous ordered moment $m_s(T \rightarrow 0) = 0.4$ Bohr magneton per Mn and a long period (180 Å) helical modulation below $T_c = 29.5$ K at ambient pressure [5]. This system has been extensively studied as a prototypical weak itinerant magnet existing near the boundary of disappearance of metallic ferromagnetism in the evolution from Fe, Ni, MnSi, to correlated paramagnet Pd, with decreasing degree of localized moment character and decreasing ordered moment size m_s relative to the effective paramagnetic moment m_p^{eff} [6]. Magnetic order in MnSi can be suppressed by application of hydrostatic pressure p above the critical pressure $p_c = 14.6$ kbar [1]. History dependence of magnetic susceptibility observed between $p^* = 12$ kbar and p_c suggests a first-order thermal phase transition at T_c in a narrow pressure region before disappearance of magnetic order. Recent neutron studies [2] have revealed existence of “partial order” spin correlations, extending over a wide pressure region at $p > p_c$ at low temperatures below T_o , whose diffusive intensity profile in reciprocal space is illustrated in Fig. 1(a). Non-zero ordered moment size at $T \rightarrow 0$, measured by Si nuclear magnetic resonance (NMR) [7, 8] up to $p = p_c$, indicates disappearance of magnetism in the first-order transition as a function of p . NMR intensity from magnetically ordered regions was found [8] to decrease with increasing p at 12 - 17 kbar. Pressure inhomogeneity in powdered NMR specimens [8], however, prevented unambiguous determinations of (a) pressure regions with spatial heterogeneity, and (b) the relationship of this phenomenon to the partial order behavior.

With its unique sensitivity to slow spin fluctuations and to signals both from paramagnetic and ordered volume fractions, muon spin relaxation (μSR) [9, 10] is a probe well suited to shed new light on magnetic behaviors around QPT. Following earlier μSR studies of MnSi in ambient pressure [11, 12, 13], we explored the crossover

region with $p = 10 - 16$ kbar using a single crystal specimen in a standard piston type pressure cell with a backward muon beam of momentum 103 MeV/c from the M9 muon channel at TRIUMF. Typically $\sim 30\%$ of the muons stopped in the specimen, of 6 mm in diameter and 10 mm long, while 70% in the wall of the pressure cell, of 23 mm in outer diameter. To assure temperature homogeneity, we used a gas-flow cryostat and two independent thermometers located at the top/bottom of the pressure cell, whose reading matched typically within ± 0.1 K.

In single crystal specimens of ordered magnetic systems, measurements in a weak transverse field (WTF) is the best way to obtain μ SR signals from a paramagnetic volume fraction. Figure 1(b) shows the precession signal and its envelope function observed in WTF = 100 G in $p = 15$ kbar at $T = 50$ K and 2.5 K. (Technical details of μ SR data processing are described in the attached “method” section.) The nearly identical signal at these two temperatures indicate that 100% of the volume is paramagnetic at $T = 2.5$ K in this pressure. At $p = 9.6$ kbar, as shown in Fig. 1(c), the envelope exhibits a clear reduction with decreasing temperature, caused by the missing signal from the magnetically ordered region of the specimen. The pressure dependence of the signal at $T = 2.5$ K in Fig. 1(d) shows that the volume fraction of the magnetically ordered region increases with decreasing pressure. From earlier μ SR studies, it is known that 100% of the volume shows magnetic order below T_c in ambient pressure with rather large internal fields (0.9 kG and 2.1 kG) at muon sites at low temperatures [12]. Thus, the envelope signals for $p = 0$ and 9.6 kbar in Fig. 1(d) represents muons stopped in the pressure cell.

By subtracting this background signal from the observed envelope, we can obtain the WTF signal from the paramagnetic region of the specimen, from which the volume fraction V_M of the region with static magnetic order was derived. Temperature and pressure dependence of V_M is shown in Fig. 2(a) and (b). In the pressure region between $p = 11.7$ kbar ($\sim p^*$) and 13.9 kbar, the static magnetic order remains in a partial volume fraction at $T \rightarrow 0$, and the ordered region completely disappears at $p = 15$ kbar, which is slightly above $p_c = 14.6$ kbar. The frequency of spontaneous muon spin precession from the magnetically ordered volume, determined in separate zero-field μ SR measurements, remain finite below 13.9 kbar, as shown in Fig. 2(b). These results indicate that the region between p^* and p_c is associated with phase separation between ordered and paramagnetic volumes, while there is no volume with static magnetism above p_c . Static magnetism with Mn spin component $> 0.004 \mu_B/\text{Mn}$, either in ferromagnetic or spin glass like correlations, would have produced static internal magnetic field > 10 G (significantly larger than the nuclear dipolar fields ~ 4 G from Mn). This situation should have lead to a distinguishable difference between $T = 50$ K and 2.5 K data in Fig. 1(b), and thus can be ruled out by the

present data.

To study dynamic spin fluctuations, we also performed measurements of the muon spin relaxation rate $1/T_1$ in a longitudinal field (LF) of 200 G. As shown in Fig. 2(c), the relaxation rate at $p \sim 1$ kbar exhibits a divergent behavior, reproducing earlier results in ambient pressure [11, 12, 13]. The critical behavior becomes less pronounced with increasing pressure. At $p = 12.7$ kbar between p^* and p_c , the anomaly of $1/T_1$ at T_c completely disappears, and the relaxation rate becomes smaller than our detection limit (dotted line in Fig. 2(c)) at $p_c < p$. In systems having magnetic order in a full volume fraction, the asymmetry of the LF- μ SR signal becomes 1/3 below T_c as shown for the results at $p = 8.0$ kbar. The asymmetry at $p = 12.7$ kbar at $T \rightarrow 0$ is significantly larger than 1/3, indicating that the magnetic order occurs only in a partial volume fraction, thus confirming the results in WTF. The full amplitude LF signal at $p = 16.3$ kbar confirms that there is no volume of magnetically ordered region above p_c .

The absence of any observable relaxation puts a severe limit for the time scale of dynamic spin fluctuations of the “partial order” spin correlations. To estimate the rate ν of this fluctuation, here we use a well known formula, $1/T_1 \sim (\gamma_\mu \times H)^2/\nu$, where H denotes the local field strength, and $\gamma_\mu = 2\pi \times 1.36 \times 10^4$ /sG is the gyromagnetic ratio of the muon spin. For a trial value of $H \sim 500$ G expected for the Mn spin polarization of $\sim 0.2 \mu_B$, the lowerlimit of $\nu > 1.2 \times 10^{10}$ /s is given by the upper limit $1/T_1 < 0.15 \mu\text{s}^{-1}$ indicated by the absence of relaxation in WTF- μ SR at $p = 15.0$ kbar at $T=2.5$ K. Similarly, the (safe) upper limit $1/T_1 < 0.05 \mu\text{s}^{-1}$, observed in LF- μ SR at 16 kbar at $T=2.9$ K, indicates $\nu > 3.6 \times 10^{10}$ /s. Although it is difficult to obtain a precise value of H for the partial order correlations, the above values serve as a reasonable estimate for the order of magnitude of ν from μ SR. Neutron scattering signals from the partial order were detected in a quasi-elastic scan with the energy resolution of 50 μeV [2], which selects static (quasi-elastic) versus dynamic responses with the fluctuation rate of 10^{11} /sec. Thus, the combination of neutron and present μ SR results indicate that the “partial order” spin correlations have dynamic character of a time scale between 10^{-11} and 10^{-10} s.

Since one might expect an influence of helical modulation in the case of MnSi, we also performed μ SR measurements in metallic $(\text{Sr}_{1-x}\text{Ca}_x)\text{RuO}_3$ system in ambient pressure, using ceramic specimens and a surface muon beam at TRIUMF. The unsubstituted SrRuO_3 exhibits a ferromagnetic order with $T_c \sim 160$ K and the ordered moment $m_s \sim 0.8 \mu_B$ per Ru at $T \rightarrow 0$. With increasing Ca concentration x , both T_c and m_s decrease, and ferromagnetic order disappears at $x \sim 0.7$, while the paramagnetic effective moment $m_p^{eff} \sim 3.0 \mu_B$ /Ru remains nearly unchanged between $x = 0$ and 1 [14]. This is a typical behavior expected in the Self Consistent Renormaliza-

tion (SCR) theory of Moriya and co-workers developed for weak ferromagnetism of itinerant electron systems [6]. Figure 3(a) shows time spectra of muon spin polarization observed in zero field at $T \sim 2\text{K}$ for specimens with various Ca concentrations. For $x = 0$ and 0.5, we see a fast damped oscillation of 2/3 of the asymmetry followed by a slowly relaxing 1/3 component, which is expected for systems having magnetic order in 100 % of the volume. The absence of long-lived muon precession is due to magnetic domain structures in ceramic specimens [15]. The spectra for $x = 0.65$ and 0.7 exhibit a slower damped oscillation, followed by increased slow-decay component, indicating that the magnetic order occurs in a partial volume fraction. No clear signature of magnetic order can be seen for $x = 0.8$ and 1.0 systems.

Figure 3(b) shows the local field width Δ , derived from the damped oscillation signal, which is proportional to the ordered moment size within the magnetically ordered volume. More data for around $x = 0.7$ is needed to determine whether $\Delta(T \rightarrow 0)$ changes abruptly or continuously as a function of x . The volume fraction V_f of the magnetically ordered region is shown in Fig. 3(c), which clearly demonstrates phase separation between ordered and paramagnetic regions at a narrow concentration range before disappearance of ferromagnetism. The product of the local moment size and the volume fraction, shown in Fig. 3(d), scales with bulk magnetization which reflects the volume integrated quantity. We have also performed $1/T_1$ measurements in ZF- μSR in $(\text{Sr}_{1-x}\text{Ca}_x)\text{RuO}_3$. The slope of T_1 versus $1/T$ above T_c , which signifies the strength of the critical divergence of the relaxation rate [11, 13], is reduced with increasing x and becomes nearly 0 at $x \sim 0.7$, indicating that the dynamic critical behavior is suppressed near QPT. The μSR results of phase separation and suppression of critical dynamics in $(\text{Sr}_{1-x}\text{Ca}_x)\text{RuO}_3$ exhibit striking resemblance to those in MnSi, which suggests a possibility that these features may be generic to QPTs in itinerant ferro/helium magnets.

We now explore quantum crossover behaviors from magnetically ordered (or superconducting) to disordered states in other correlated electron systems. Table 1 lists known cases where the crossover is associated with either a first-order transition (FOT) or phase separation (PS) or partial volume fraction of the ordered region (PVF). Note that volume integrated measurements, such as bulk magnetization or neutron scattering, allow distinction of FOT only when an abrupt change is detected at the phase boundary. Continuous change in these measurements can be due either to a true second order phase transition or to a FOT accompanied by PS where the product of moment size and volume fraction exhibits a continuous variation as in Fig. 3(d). In contrast, NMR/NQR and μSR can distinguish signals from ordered and disordered volumes. When single crystal specimens are available, μSR has the further advantage of avoiding pressure/system

heterogeneities due to powdered specimens. Table 1 demonstrates that many of known cases of crossover, not only in itinerant magnets but also in heavy-fermion and high- T_c systems, are associated with FOT/PS/PVF. It fact, it is not easy to find a well-established case of a QPT in such systems with a truly second order transition.

In his pioneering theoretical contribution which initiated modern discussions of QPT, Hertz [16] mapped QPT to thermal counterparts in a higher effective dimension, and thus expected a better applicability of mean-field theory and second order transitions in quantum transitions. Contrary to this expectation, many actual systems exhibit first order transitions. Figure 4 illustrates the evolution of the free energy as a function of order parameter in typical second order ((a) and (b)) and first order phase transitions ((c) and (d)). Recently, Belitz *et al* [17] ascribed first order transition in itinerant ferromagnets to terms in free energy arising from coupling of low energy spin fluctuation modes and order parameter fluctuations, which leads to a free energy profile similar to that shown by the (c) line in Fig. 4 at T_c . Alternatively, first order QPTs with such free energy profile could also be due, in general, to effects of band structure in metallic ferromagnets. Randomness would suppress low energy fluctuations and/or smear out discontinuous changes, thus favouring tendency towards apparent second order transition in both cases. Clear observation of PS in $(\text{Sr}_{1-x}\text{Ca}_x)\text{RuO}_3$, overcoming possible effects of randomness in chemically substituted systems, can then be taken as a rather robust evidence against second order transition. Although FOT and PS are not necessarily the identical concepts, PS is associated with FOT in the majority of the cases. In general, when the relevant energy scale is lowered near a QPT, a competing phenomenon, such as superconductivity in UGe_2 , and/or a generic tendency towards first order transition become a dominant factor, winning over the simpler scheme initially proposed by Hertz. This provides a natural way to understand overwhelming tendency towards FOT/PS/PVF shown in Table 1.

As a novel type of spin correlation at QPT, the partial order correlations of MnSi have become a focus of theoretical interest, and several different models have been presented for their explanation, such as “helical spin crystals” [18], “blue quantum fog” [19], “skyrmion state” [20], as well as “magnetic rotons” [21]. The magnetic roton model views the partial order correlations as a manifestation of a spin soft mode towards helical spin order, analogous to rotons in superfluid He, which crosses over to solid helium with increasing pressure at $p \sim 26$ bar via first-order QPT [22]. These correlations may also be analogous to the 41 meV neutron resonance mode in the cuprate systems [23, 24] heading towards the stripe spin/charge ordered state. By revealing the dynamic nature of the partial order correlations, and providing their

energy/time scale 10^{10-11} /s, the present results give severe constraints to future development of these models / theories.

In summary, we have presented μ SR studies on dynamic and static magnetic behaviors at QPTs of MnSi and (Sr,Ca)RuO₃, which demonstrate spontaneous phase separation and suppression of dynamic critical behavior. It is interesting to note that nearly identical spin responses are observed in MnSi which involves low crystal symmetry and Dzyaloshinskii-Moriya interaction [25] and in (Sr,Ca)RuO₃ having higher symmetry and ferromagnetic ground state. These findings, together with other known cases in heavy-fermion and cuprate systems, promote the development of a comprehensive understanding of QPT in correlated electron systems which clarifies the role of first order transitions.

We acknowledge financial supports from NSF DMR-05-02706 (Material World Network, Inter-American Materials Collaboration programme) at Columbia and Kentucky, NSF DMR-01-02752 and CHE-01-11752 at Columbia, NSERC and CIAR (Canada) at McMaster, Brazilian grant CIAM-CNPq 49.2674/2004-3 at CBPF, and CIAM-CONICET project 509/20-04-05 at CAB Bariloche, Argentina; technical supports from S.R. Kreitzman and K. Satoh; and scientific discussions with B. Binz, M. Continentino, S.R. Julian, and A.J. Millis.

Method

In μ SR [9] in a transverse field, the time spectrum from a paramagnetic / nonmagnetic specimen (and pressure cell) is given by

$$N(t) = N_o \exp(-t/\tau_\mu)[1 + AG(t) \cos(\gamma_\mu H_{ext}t + \phi)],$$

where $\tau_\mu = 2.2\mu$ s is the muon lifetime, $\gamma_\mu = 2\pi \times 13.6$ kHz/G is the gyromagnetic ratio of the muon spin, $A \sim 0.2-0.3$ is the initial asymmetry (constant for a given spectrometer / beamline condition), $G(t)$ is the relaxation function, H_{ext} is the magnitude of static external field (plus Knight shift) at the muon site, and ϕ is the initial phase of precession (which depends on the location of the counter). When some volume undergoes static magnetic order, producing a static internal field H_{int} at the muon site, the oscillation amplitude for the frequency $\gamma_\mu H_{ext}$ is reduced. In the case of MnSi below T_c , where the vector sum of H_{ext} ($= 100$ G) and H_{int} (≥ 900 G at $T \rightarrow 0$ and $p = 0$) has a wide spread (~ 100 G or more) in magnitude, the oscillating signal from the magnetically ordered volume is depolarized within $t = 100$ ns or less. As a display of the response from para/non-magnetic volume, Fig. 1(b) shows the raw data $|AG(t) \cos(\gamma_\mu H_{ext}t + \phi)|$, together with the “envelope” $AG(t)$ obtained by dividing the data with the cosine function (we avoided plotting the time region where the cosine function is close to zero). By fitting the amplitude of this cosine signal, assuming a slowly decaying function for $G(t)$ (due mostly to nuclear dipolar fields), we

obtained the fraction of muons stopped in the paramagnetic region of MnSi plus the non-magnetic pressure cell. The cell contribution was calibrated using the data at $T = 2.5$ K at ambient pressure, where the full volume of MnSi is known to undergo static order. Subtracting this cell amplitude, we obtained the precession amplitude of muons representing the “paramagnetic volume fraction of MnSi”, from which the plot in Fig. 2(a) was constructed. In zero-field (ZF) or longitudinal-field (LF) μ SR, the time histograms for the forward (F) / backward (B) counters are given as

$$N_{F/B}(t) = N_{Fo/Bo} \exp(-t/\tau_\mu)[1 \pm AG(t)].$$

The relaxation function $G(t)$ describes the time evolution of muon spin polarization from the initial value of $G(t = 0) = 1.0$. Full relaxation makes $G(t) = 0$. For signals from multiple different regions, such as the cell and the specimen, $G(t)$ is decomposed into additive signals from different regions. In paramagnetic systems, the sample signal usually exhibits an exponential decay $\exp(-t/T_1)$, while in the ordered state in ZF one observes a damped oscillation of the 2/3 of the asymmetry added to a slow decay of the 1/3 asymmetry, which represents muons at the sites with the internal field from ordered moments being rather parallel to the initial muon polarization, as seen in $G(t)$ for $x < 0.5$ at low temperatures in Fig. 3(a). This 2/3:1/3 ratio could depend on crystal orientation for single crystal specimens, as well as the ratio between external and internal field in LF. For cubic crystal of MnSi which has eight [111] spiral directions, however, we expect that a balanced random population of domain orientations at low/zero field would minimize the orientation effect, leading to nearly 2:1 ratio similar to the case for powder/ceramic samples. The asymmetry plotted in Fig. 2(c) corresponds to the relative magnitude of the non-oscillating component within the signal from the MnSi specimen, after the background signal from the pressure cell was subtracted.

-
- [1] C. Pfleiderer, G. J. McMullan, S. R. Julian, and G. G. Lonzarich, Magnetic quantum phase transition in MnSi under hydrostatic pressure, Phys. Rev. **B 55** (1997) 8330 - 8338.
 - [2] C. Pfleiderer, D. Reznik, L. Pintschovius, H.v. Löhneysen, M. Garst, A. Rosch, Partial order in the non-Fermi-liquid phase of MnSi, Nature **427** (2004) 227 - 231.
 - [3] C. Pfleiderer, M Uhlarz, S M Hayden, R Vollmer, H. v. Löhneysen, N. R. Bernhoeft, G. G. Lonzarich, Coexistence of superconductivity and ferromagnetism in the d-band metal ZrZn₂, Nature **412** (2001) 58-61.
 - [4] S.S. Saxena, P. Agarwal, K. Ahilan, F.M. Grosche, R.K.W. Haselwimmer, M.J. Steiner, E. Pugh, I.R. Walker, S.R. Julian, P. Monthoux, G.G. Lonzarich, A. Huxley, I. Sheikin, D. Braithwaite, J. Flouque, Super-

- conductivity on the border of itinerant-electron ferromagnetism in UGe₂, *Nature* **406** (2000) 587-592.
- [5] Y. Ishikawa, G. Shirane, J. A. Tarvin, and M. Kohgi, Magnetic excitations in the weak itinerant ferromagnet MnSi, *Phys. Rev.* **B16** (1977) 4956-4970.
- [6] T. Moriya, **Spin Fluctuations in Itinerant Electron Magnetism**, Springer Series in Solid State Science **56**, (Springer, Heidelberg, 1985), and references therein.
- [7] C. Thessieu, Y. Kitaoka and K. Asayama, Magnetic quantum phase transition in MnSi, *Physica* **B259-261** (1999) 847-848.
- [8] W. Yu, F. Zamborszky, J.D. Thompson, J.L. Sarrao, M.E. Torelli, Z. Fisk, and S.E. Brown, Phase Inhomogeneity of the Itinerant Ferromagnet MnSi at High Pressures, *Phys. Rev. Lett.* **92** (2004) 086403 [4 pages].
- [9] For a recent reviews of μ SR studies in topical subjects and technical aspects of μ SR, see *Muon Science: Muons in Physics, Chemistry and Materials*, Proceedings of the Fifty First Scottish Universities Summer School in Physics, St. Andrews, August, 1988, ed. by S.L. Lee, S.H. Kilcoyne, and R. Cywinski, Inst. of Physics Publishing, Bristol, 1999.
- [10] A.T. Savici, Y. Fudamoto, I.M. Gat, T. Ito, M.I. Larkin, Y.J. Uemura, G.M. Luke, K.M. Kojima, Y.S. Lee, M.A. Kastner, R.J. Birgeneau, K. Yamada, Muon spin relaxation studies of incommensurate magnetism and superconductivity in stage-4 La₂CuO_{4.11} and La_{1.88}Sr_{0.12}CuO₄, *Phys. Rev.* **B66** (2002) 014524.
- [11] R.S. Hayano, Y.J. Uemura, J. Imazato, N. Nishida, T. Yamazaki, H. Yasuoka, and Y. Ishikawa, Observation of the $T/(T - T_c)$ Divergence of the μ^+ Spin-Lattice Relaxation Rate in MnSi near T_c , *Phys. Rev. Lett.* **41** (1978) 1743 - 1746.
- [12] R. Kadono, T. Matsuzaki, T. Yamazaki, S.R. Kretziman, and J.H. Brewer, Spin dynamics of the itinerant helimagnet MnSi studied by positive muon spin relaxation, *Phys. Rev.* **B42** (1990), 6515-6522.
- [13] I.M. Gat-Malureanu, A. Fukaya, M.I. Larkin, A.J. Millis, P.L. Russo, A.T. Savici, Y.J. Uemura, P.P. Kyriakou, G.M. Luke, C.R. Wiebe, Y.V. Sushko, R.H. Heffner, D.E. MacLaughlin, D. Andreica, and G.M. Kalvius, Field Dependence of the Muon Spin Relaxation Rate in MnSi, *Phys. Rev. Lett.* **90** (2003) 157201 [4 pages].
- [14] T. Kiyama, K. Yoshimura, K. Kosuge, H. Mitamura, T. Goto, High-Field Magnetization of Sr_{1-x}Ca_xRuO₃, *J. Phys. Soc. Japan* **68** (1999) 3372-3376.
- [15] Ch. Niedermayer, private communication, 2006.
- [16] J.A. Hertz, Quantum critical phenomena, *Phys. Rev.* **B14** (1976) 1165-1184.
- [17] D. Belitz, T. R. Kirkpatrick, and J. Rollbühler, Tricritical Behavior in Itinerant Quantum Ferromagnets, *Phys. Rev. Lett.* **94** (2005) 247205.
- [18] B. Binz, A. Vishwanath, and V. Aji, Theory of the helical spin crystal: A candidate for the partially ordered state of MnSi, *Phys. Rev. Lett.* **96** (2006) 207202.
- [19] S. Tewari, D. Belitz and T. R. Kirkpatrick, Blue quantum fog: Chiral condensation in quantum helimagnets, *Phys. Rev. Lett.* **96** (2006) 047207.
- [20] U. K. Rössler¹, A. N. Bogdanov, and C. Pfleiderer, Spontaneous skyrmion ground states in magnetic metals, *Nature* (2006), in press.
- [21] J. Schmalian and M. Turlakov, Quantum phase transitions of magnetic rotons, *Phys. Rev. Lett.* **93** (2004) 036405.
- [22] O.W. Dietrich, E.H. Graf, C.H. Huang, L. Passell, *Neutron scattering by rotons in liquid helium*, *Phys. Rev.* **A5** (1972) 1377.
- [23] Y.J. Uemura, Condensation, excitation, pairing, and superfluid density in high- T_c superconductors: magnetic resonance mode as a roton analogue and a possible spin-mediated pairing, *J. Phys. Condens. Matter* **16** (2004) S4515 - S4540.
- [24] Y.J. Uemura, Twin spin/charge roton mode and superfluid density: Primary determining factors of T_c in high- T_c superconductors observed by neutron, ARPES, and μ SR, *Physica* **B374-375** (2006) 1-8.
- [25] P. Bak and M. H. Jensen, Theory of helical magnetic structures and phase transitions in MnSi and FeGe, *J. Phys. C: Solid St. Phys.* **13** (1980) L881-5.
- [26] C. Pfleiderer and A.D. Huxley, Pressure dependence of the magnetization in the ferromagnetic superconductor UGe₂, *Phys. Rev. Lett.* **89** (2002) 147005.
- [27] A. Harada, S. Kawasaki, H. Kotegawa, Y. Kitaoka, Y. Haga, E. Yamamoto, Y. Onuki, K.M. Itoh, E.E. Haller, and H. Harima, Cooperative Phenomenon of Ferromagnetism and Unconventional Superconductivity in UGe₂: A ⁷³Ge-NQR Study under Pressure, *J. Phys. Soc. Jpn.* **74** (2005) 2675.
- [28] M. Uhlarz, C. Pfleiderer, and S. M. Hayden, Quantum Phase Transitions in the Itinerant Ferromagnet ZrZn₂, *Phys. Rev. Lett.* **93** (2004) 256404.
- [29] G.M. Luke, A. Keren, K. Kojima, L.P. Le, B.J. Sternlieb, W.D. Wu, Y.J. Uemura, Y. Onuki and T. Komatsubara, Competition between Magnetic Order and Superconductivity in CeCu_{2.2}Si₂, *Phys. Rev. Lett.* **73** (1994) 1853-1856
- [30] K. Matsuda, Y. Kohori, T. Kohara, K. Kuwahara, and H. Amitsuka, Spatially Inhomogeneous Development of Antiferromagnetism in URu₂Si₂: Evidence from ²⁹Si NMR under Pressure, *Phys. Rev. Lett.* **87** (2001) 087203 (2001)
- [31] G.M. Luke, A. Keren, L.P. Le, W.D. Wu, Y.J. Uemura, D. Bonn, L. Taillefer, J.D. Garrett, Y. Onuki, Muon Spin Relaxation in Heavy Fermion Systems, *Hyperfine Interact.* **85** (1994) 397-409.
- [32] H. Amitsuka, M. Yokoyama, S. Miyazaki, K. Tenya, T. Sakakibara, W. Higemoto, K. Nagamine, K. Matsuda, Y. Kohori and T. Kohara, Hidden order and weak antiferromagnetism in URu₂Si₂, *Physica B* **312-313** (2002) 390-396.
- [33] Y. Kitaoka, S. Kawasaki, T. Mito, Y. Kawasaki, Unconventional Superconductivity in Heavy Fermion Systems, *J. Phys. Soc. Japan* **74** (2005) 186, and reference therein.
- [34] B. Nachumi, A. Keren, K. Kojima, M. Larkin, G.M. Luke, J. Merrin, O. Tchernyshov, Y.J. Uemura, N. Ichikawa, M. Goto, and S. Uchida, Muon Spin Relaxation Studies of Zn-Substitution Effects in High- T_c Cuprate Superconductors, *Phys. Rev. Lett.* **77** (1996) 5421-5424.
- [35] S.H. Pan, E.W. Hudson, K.M. Lang, H. Eisaki, S. Uchida, J.C. Davis, Imaging the Effects of Individual Zinc Impurity Atoms on Superconductivity in Bi₂Sr₂CaCu₂O_{8+ δ} , *Nature (London)* **403** (2000) 746.
- [36] K.M. Kojima, S. Uchida, Y. Fudamoto, I.M. Gat, M.I. Larkin, Y.J. Uemura, G.M. Luke, Superfluid density and volume fraction of static magnetism in stripe-stabilized La_{1.85-y}Cu_ySr_{0.15}CuO₄, *Physica B* **326** (2003) 316-320.
- [37] H.E. Mohottala, B.O. Wells, J.I. Budnick, W.A. Hines, Ch. Niedermayer, L. Udby, C. Bernhard, A.R. Moodenbaugh, F.-C. Chou, Phase separation in superoxygenated

- $\text{La}_{2-x}\text{Sr}_x\text{CuO}_{4+y}$, *Nature Materials* **5** (2006) 377-382.
- [38] Y.J. Uemura, A. Keren, L.P. Le, G.M. Luke, W.D. Wu, Y. Kubo, T. Manako, Y. Shimakawa, M. Subramanian, J.L. Cobb, and J.T. Markert, Magnetic Field Penetration Depth in $\text{Tl}_2\text{Ba}_2\text{CuO}_{6+\delta}$ in the Overdoped Regime, *Nature* **364** (1993) 605-607.
- [39] J.C. Seamus Davis, private communication (2005).

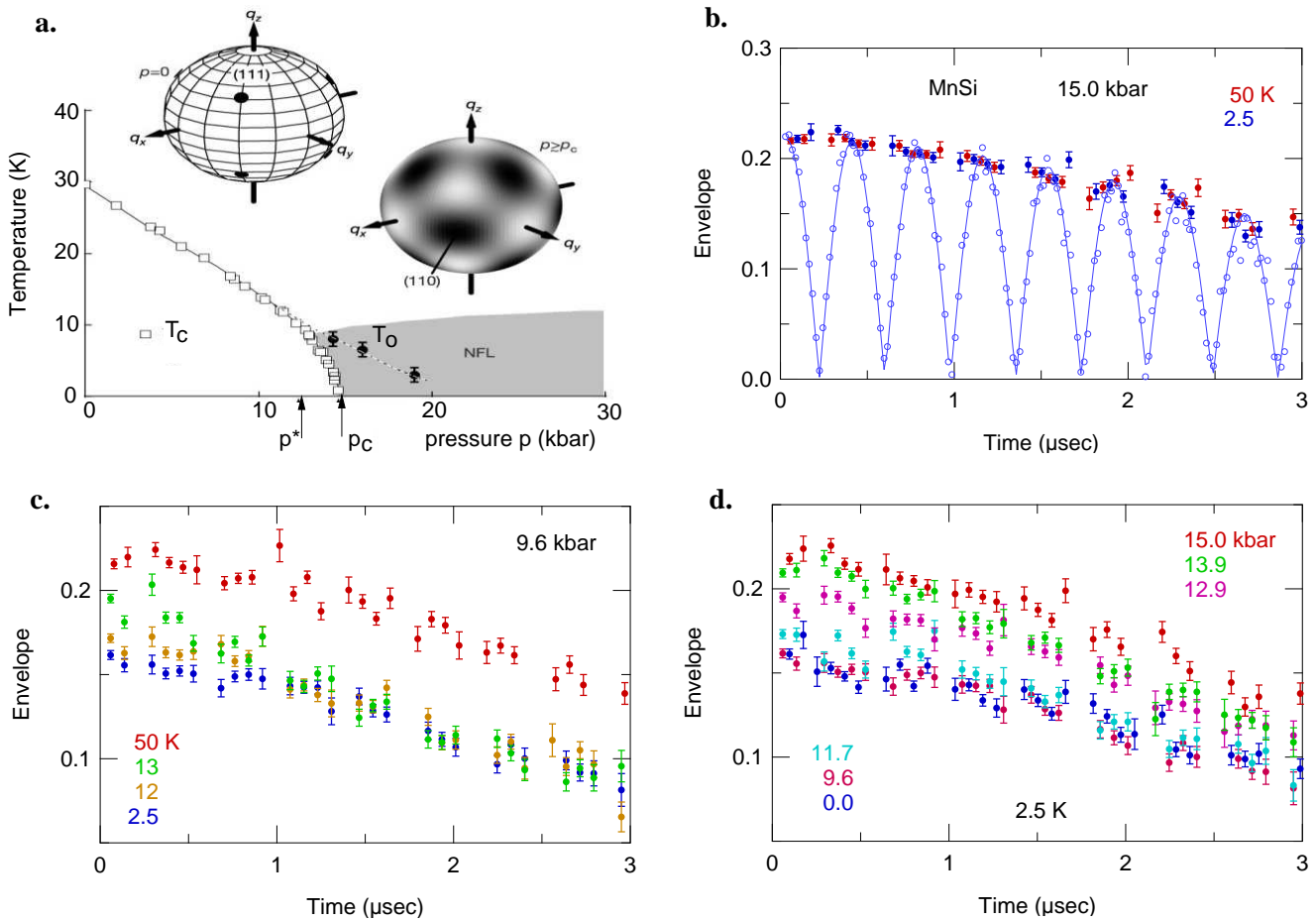


FIG. 1: (color) (a) Phase diagram of MnSi as a function of pressure [2]. History dependent behavior has been found between $p^* \sim 12$ and $p_c = 14.6$ kbar. The closed circles show a temperature T_0 below which a diffuse neutron scattering intensity, illustrated in a right intensity-map sphere, was observed. The shaded region exhibits a non-Fermi-liquid behavior in transport measurements. (b) Muon spin precession pattern observed in a single crystal specimen of MnSi within a pressure cell in a weak transverse external field (WTF) of 100 G, and the envelope of the oscillation spectra at $T = 50$ K and 2.5 K at $p = 15$ kbar. The amplitude of this envelope represents muons in the non-magnetic or paramagnetic environment. No difference between $T = 50$ K and 2.5 K indicates absence of static magnetic order at $T = 2.5$ K at a pressure slightly above p_c . (c) Temperature dependence of the envelope at $p = 9.6$ kbar. The reduction of the precessing envelope is caused by the volume of the specimen which has undergone static magnetic order. The envelope observed at $T = 2.5$ K represents muons stopped in the pressure cell, after the signal from ordered MnSi being quickly depolarized. (d) Pressure dependence of the envelope at $T = 2.5$ K. At ambient pressure and 9.6 kbar, 100 % of the volume of MnSi undergoes static magnetic order, while the static magnetic order takes place in a reduced volume fraction between $p = 11.7$ and 13.9 kbar.

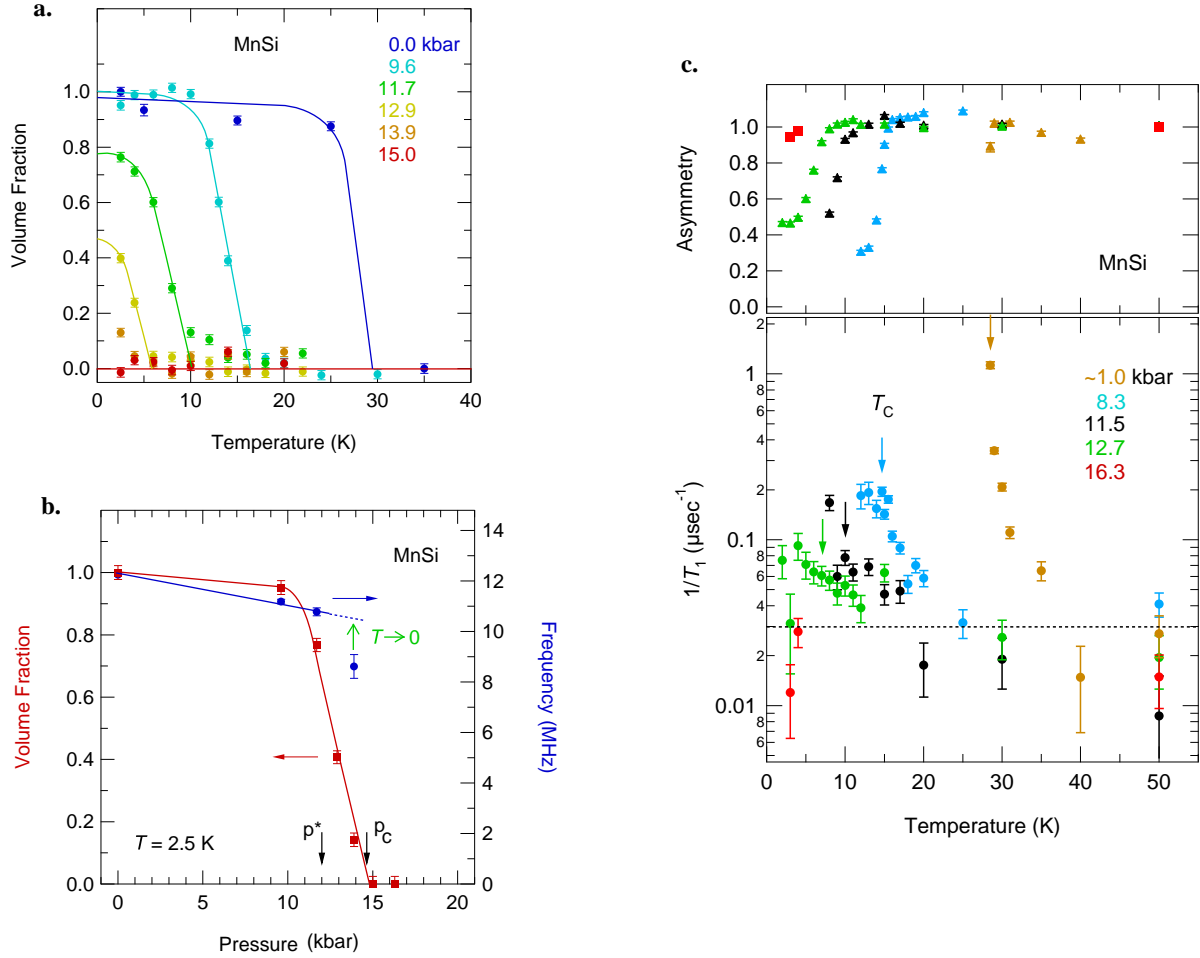


FIG. 2: (color) (a) Temperature and pressure dependences of the volume fraction V_M having static magnetic order in MnSi determined from the muon precession envelope measured in WTF of 100 G. The volume fraction remains finite at $T \rightarrow 0$ at the pressure p between 11.7 and 13.9 kbar, indicating phase separation between magnetically ordered and paramagnetic volumes. (b) Pressure dependence of the ordered volume fraction, determined in WTF of 100 G, and the muon spin precession frequency observed in zero-field μSR , at $T = 2.5$ K. The finite frequency near p_c indicates a first order phase transition. The frequency at $p = 13.9$ kbar at $T = 2.5$ K $\sim 0.5 T_c$ is expected to increase at $T \rightarrow 0$ as illustrated by the green arrow. (c) The muon spin relaxation rate $1/T_1$ and the relaxing muon asymmetry obtained in μSR measurements in a longitudinal field (LF) of 200 G. Divergent critical behavior of $1/T_1$, seen at $p \sim 1$ kbar, is gradually suppressed with increasing pressure. No anomaly of $1/T_1$ is seen at T_c (indicated by arrows) at $p = 12.7$ kbar, between p^* and p_c . At $p = 16.3$ kbar, $1/T_1$ becomes smaller than the technical limit of detection, indicated by the broken line.

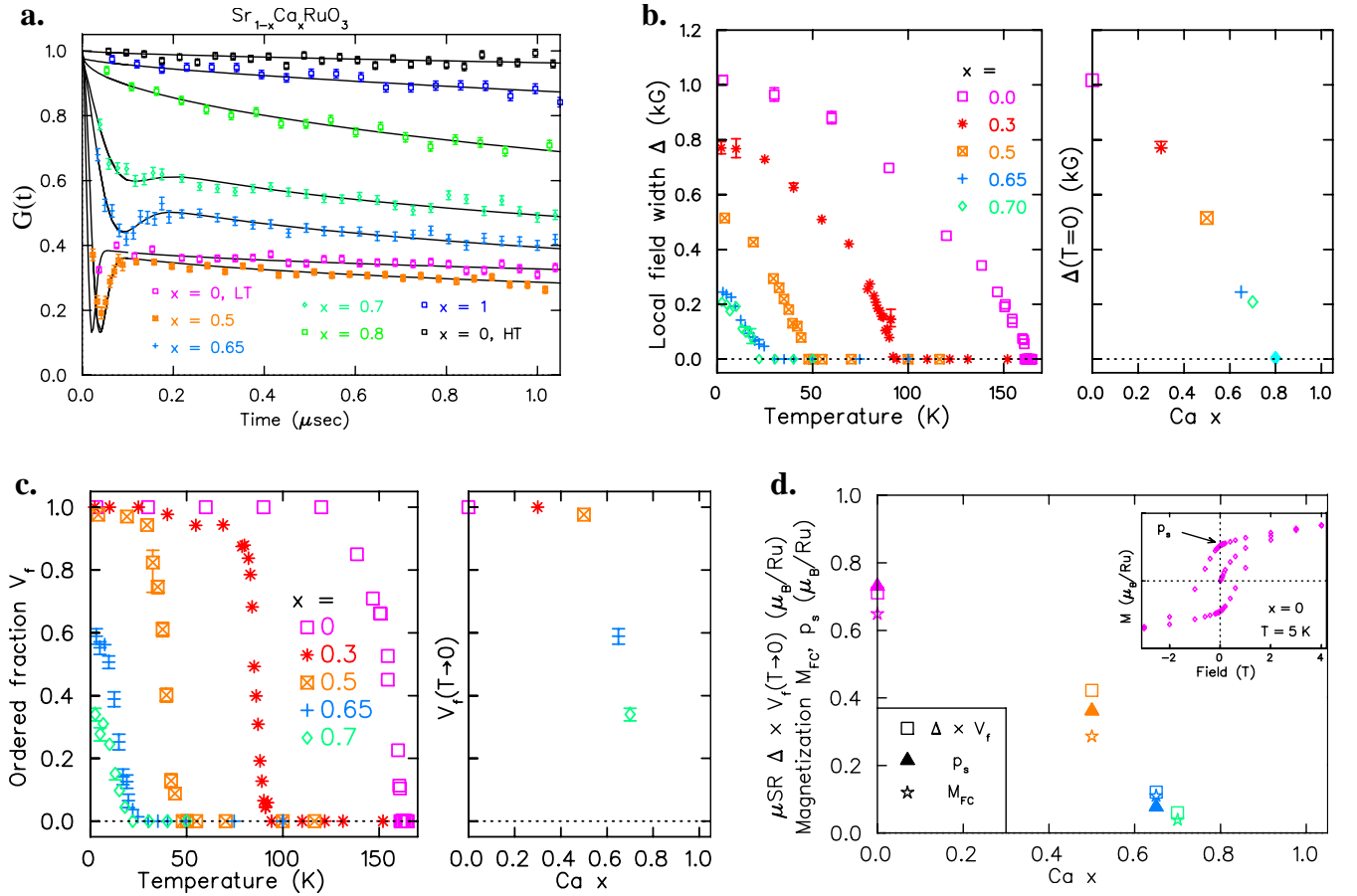


FIG. 3: (color) (a) Muon spin relaxation spectra observed in zero field in $(\text{Sr}_{1-x}\text{Ca}_x)\text{RuO}_3$ at $T \sim 2.5 - 5$ K (indicated as LT) in ceramic specimens of various x , compared with that at $T = 164$ K (HT) in SrRuO_3 above T_c . The LT spectra shows a damped oscillation with the amplitude of $2/3$, expected for static order in full volume, in $x = 1.0$ and 0.5 . Reduced amplitude is seen for $x = 0.65$ and 0.7 , indicating a finite volume fraction of magnetically ordered region. The oscillation is replaced by a slow relaxation in $x = 0.8 - 1.0$. The solid line represents a fit to a Gaussian Kubo-Toyabe function multiplied by an exponential decay. (b) Temperature and concentration dependence of the amplitude Δ of static random local field, derived from the fit of ZF- μSR data to the Gaussian Kubo Toyabe function, in $(\text{Sr}_{1-x}\text{Ca}_x)\text{RuO}_3$. The width Δ is proportional to the average size of static ordered moment in the magnetically ordered volume. Note that $\Delta(T \rightarrow 0)$ shows a marked reduction from $x = 0.7$ to 0.8 . (c) Volume fraction V_f of the magnetically ordered region determined by ZF- μSR in $(\text{Sr}_{1-x}\text{Ca}_x)\text{RuO}_3$. For $x > 0.7$, the damped oscillation is replaced by a slow relaxation, which suggests disappearance of the volume having ordered moment greater than $m_s \sim 0.01 \mu_B$ per Ru. (d) Comparison of $\Delta \times V_f(T \rightarrow 0)$ by μSR to magnetization measured in field cooling (M_{FC}) and the spontaneous moment p_s seen in the field-cycling, as illustrated in the inset, all measured at low temperatures (2-5) K. The latter two quantities represent the volume integrated response. Reasonable agreement of those with the product of Δ and V_f further confirms phase separation before static magnetism disappears around $x \sim 0.7$.

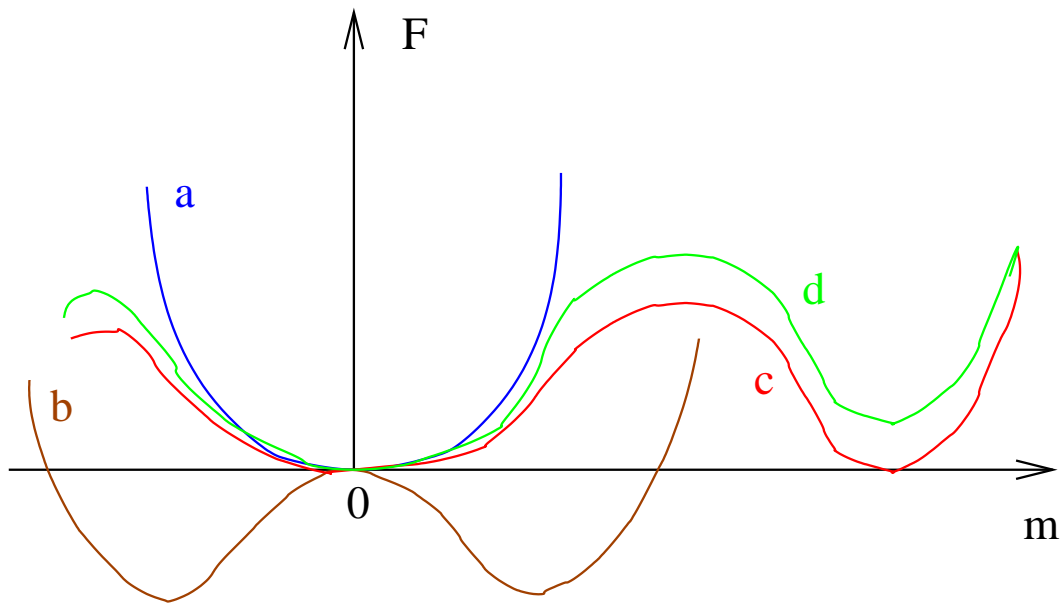


FIG. 4: (color) A schematic view of free energy F , as a function of magnetic order parameter m , illustrated for the second order phase transition in the disordered state (line (a)); and the ordered state (line (b)); and the first order phase transition at the ordering temperature or pressure (line ((c)) and in the disordered state near the ordering (line(d)). A discussion for the situation with line (c) in itinerant ferromagnets has been given by Belitz *et al.* [17].

TABLE I: Phase Separation (PS) / First-Order Transition (FOT) / Partial-Volume (PVF) features detected at QPT

System	Crossover	Parameter (p in kbar)	FOT/PS/PVF	Method	Ref.	Remark, [Limitation]
<i>Itinerant electron magnets</i>						
UGe ₂	FM1-Para	$p_c=16$	FOT PS	Magnetization Ge-NQR	[26] [27]	Sudden drop coexist signal [powder]
ZrZn ₂	Ferro-Para	$p_c = 16.5$	FOT	Magnetization	[28]	Sudden drop
MnSi	Helical-Para	$12=p^* < p < p_c=14.6$ $p < p_c$ $p < 18$ $p^* < p < p_c$	FOT FOT PVF PS FOT	Susceptibility Si-NMR Si-NMR μ SR	[1] [7] [8] Present Work	sharp change [powder] intensity drop [powder] volume fraction, x-tal suppressed critical dynamics
(Sr _{1-x} Ca _x)RuO ₃	Ferro-Para	$0.7 < Ca(x) < 0.65$	PS FOT	μ SR	Present Work	volume fraction suppressed critical dynamics
<i>Heavy Fermion Systems</i>						
CeCu _{2.2} Si ₂	AF(a)-SC	Temp.	PS	μ SR	[29]	AF volume change at SC
URu ₂ Si ₂	AF-Hidden	$3 < p < 10$ $0 < p < 10$	PVF PVF/FOT	Si-NMR μ SR	[30] [31, 32]	[hidden order missing]
CeIn ₃	AF-SC	$p_c=24.3$	FOT	In-NQR	[33]	FOT also in FM-PM
<i>High-T_c systems</i>						
(La,Sr) ₂ (Cu _{1-x} Zn _x)O ₄	SC-normal	Zn(x)	PS	μ SR	[34]	Swiss Cheese model
Bi ₂ Sr ₂ Ca(Cu _{2-x} Zn _x)O ₈	SC-normal	Zn(x)	PS	STM	[35]	normal region around Zn
(La _{1.85-y} Sr _{0.15} Eu _y)CuO ₄	Stripe-SC	Eu(y)	PS	μ SR	[36]	volume fraction trade-off
O-doped (La _{2-x} Sr _x)CuO _{4+y}	Stripe-SC	Temp., Sr(x)	PVF/PS	μ SR	[10, 37]	stripe islands[10]
Tl ₂ Ba ₂ CuO _{6+δ}	SC-Metal	overdope O(δ)	PS	μ SR	[23, 38]	boson-fermion coexistence
Bi ₂ Sr ₂ CaCu ₂ O _{8+δ}	SC-Metal	overdope O(δ)	PS	STM	[39]	inhomogeneous gap closing

SC denotes superconducting phase, STM denotes Scanning Tunnelling Microscope.